Revealing Origin of Hydrogen-Carbonate Species in CO Oxidation Over Pt/Al2O3: A SSITKA-IR Study

Ibrahim Hatoum, Nassim Bouchoul, Mélissandre Richard, Christophe Dujardin

Revealing origin of hydrogen-carbonate species in CO oxidation over Pt/Al_2O_3: a SSITKA-IR study

Ibrahim Hatoum*[1], Nassim Bouchoul[1], Mélissandre Richard[1], Christophe Dujardin [1]

[1] *Univ. Lille, CNRS, Centrale Lille, Univ. Artois, UMR 8181, UCCS - Unité de Catalyse et Chimie du Solide, 59000 Lille, France*

Abstract The catalytic oxidation of CO by O_2 to form CO_2 over Pt based catalysis is one of the most studied catalytic reaction leading to controversial mechanism descriptions. Steady State Isotopic Transient Kinetic Analysis (SSITKA) coupled with InfraRed (IR) spectroscopy is a powerful technique to study heterogeneous reaction mechanisms combining both the observation of adsorbed species on the catalyst surface and kinetic measurements. In this paper, SSITKA-IR technique was applied to study the CO oxidation reaction in presence and absence of CO_2 in order to distinguish between active and spectator intermediates formed during the reaction. Linear carbonyl and bridged carbonyl type species adsorbed on metallic Pt^0 were clearly identified as active intermediates at low temperature (131 °C). In contrast, the hydrogen-carbonate species formed during CO oxidation reaction were proven to be inactive species in CO_2 formation but rather due to the re-adsorption of CO_2 product itself on alumina surface.

Keywords CO oxidation · SSITKA · *Operando* IR spectroscopy · Hydrogen-carbonate · Mechanism

Introduction

Air pollution, along with climate change, is one of the most serious environmental threats to human health responsible for 7 million premature deaths per year and loss of millions healthy life years [1]. Transportation industry is the largest contributor to air pollution with emissions of carbon monoxide (CO), nitrogen oxides (NO_x), unburned hydrocarbons (HC) and particulate matter [2]. In Europe, legislation imposing restrictions on the emissions of pollutants from vehicle exhaust has been introduced since 90's and the next coming Euro 7 regulations are expected to reduce drastically the acceptable emissions thresholds. Thus, one of the greatest challenges for current catalytic converter technologies will be to meet the major issue of cold-start (warm up) emissions, when catalyst has not yet reached its light-off temperature [3]. In that context, the catalytic CO oxidation at low temperature has gained increasing attention [4–6]. This reaction is one of the most extensively studied in the history of heterogeneous catalysis. Despite the fact that CO oxidation appears to be a relatively straightforward reaction, the fundamental understanding of the process over supported noble metal particles is still a matter of debate. Over 20 different mechanistic steps have been proposed [7]. The Langmuir–Hinshelwood (LH) dual-site mechanism, in which the reaction occurs between CO and O_2 after both

molecules have been adsorbed on the surface of a catalyst, is one of the most widely accepted pathway for low-temperature CO oxidation [8–10]. Recently, Newton et al. proposed a carbonatemediated mechanism for CO oxidation at low temperature over a highly dispersed γ-alumina-supported Pt catalyst [11–13]. However, the participation of carbonate and hydrogen- carbonate species is not explicitly demonstrated in the literature. The Steady State Isotopic Transient Kinetic Analysis (SSITKA) coupled with operando InfraRed spectroscopy (IR) is one of the most powerful system to investigate catalytic reaction mechanisms. The combination of steady state and isotopic transient conditions highlights the advantages of both techniques as obtaining kinetic information and identifying the structural properties of the surface-adsorbed active or inactive species at molecular level under the realistic steadystate conditions of the reaction [14, 15]. In this work, combined SSITKA-transmission IR experiments will be applied for the first time to study the oxidation of CO on Pt/Al_2O_3 catalyst unraveling the true role of hydrogen-carbonate species during the reaction at low temperature.

2 Experimental

2.1 Catalyst Preparation and Characterization

The catalyst was prepared by incipient wetness impregnation of ɣ-Al_2O_3 support (supplied by the Centre de Recherches de SOLAIZE TOTALEnergies) with platinum (II) acetylacetonate (Fluka) precursor salt to obtain 1 wt% metal loading. The sample was dried overnight at 85 °C, calcined 2 h under air flow at 500 °C (ramp 10 °C/min) and reduced with dihydrogen 2.5 h at 400 °C (ramp 5 °C/min). Final Pt loading was determined by ICP-OES 5110 (Agilent Technologies). Nitrogen physisorption measurements were performed on a Micromeritics TriStar II instrument. The experiments were conducted using 0.2 g of powder sample, previously outgazed at 150 °C under vacuum for 2 h. Brunauer-Emmett- Teller (BET) theory was applied to calculate the specific surface area. Pore size distributions were obtained from the complete isotherms based on the Barret-Joyner-Halenda (BJH) theory. H_2 chemisorption measurement was carried out at 30 °C in a Micromeritics Autochem II instrument using a pulse technique. Prior to the adsorption, the catalyst (50 mg) was preheated in pure H_2 at 400 °C and outgassed in flowing Argon at 400 °C. Then the temperature of the catalytic bed was reduced to 30 °C in order to perform the measurement in which H_2 pulses (5 vol% H_2 in Ar) were injected until saturation. Metal dispersion was calculated assuming H/Pt = 1.

2.2 SSITKA-IR Experiments

The Pt/Al_2O_3 catalyst was finely crushed and pressed into a 5.9 mg square pellet of 1.21 cm^2 under a pressure of 100 MPa for *operando* SSITKA-IR measurements. The pellet was loaded in the homemade IR cell with an internal dead volume inferior to 0.5 cm^3 and equipped with KBr windows. The cell was connected upstream to an automatic regulator for gas flow and switch valves controls. Prior to the SSITKA-IR study, the catalytic material was pre-treated at 300 °C during 5 h under He (35 mL/min).

Then, 2060 ppm CO/10% O_2/ He gas flow mixture was sent to the catalyst at a total flow rate of 12 mL/min (122 L h^{-1} g^{-1}). The temperature was increased from 50 °C up to 131 °C (1 °C/min) corresponding to a CO conversion of 11%. After 30 min of isotherm equilibration, the SSITKA-IR experiment was performed by switching the reactant from ^{12}CO to its labelled counterpart ^{13}CO at the same concentration, pressure and temperature. This $^{12}CO \rightarrow {}^{13}CO$ gas switch step was repeated three times to record the concentration evolution of reversibly adsorbed CO and active C_x intermediates but also to check reproducibility (true steady-state achieved). 5000 ppm of Kr and 7900 ppm of CH_4 were used as inert gas for kinetic analysis (i.e. SSITKA gas switching procedure: $^{12}CO/ O_2/He \rightarrow {}^{13}CO/O_2/He/Kr/CH_4$). The comparison of Kr and CH_4 mass spectrometry (MS) signals is presented in supplementary information and confirms the absence of time delay between the two gas responses (Fig. S1). The use of methane allows direct comparison of MS (gas phase) and IR (adsorbed species) signals. Finally, the catalyst was heated up to 300 °C (1 °C/min) before cooling it down to 50 °C. The SSITKA-IR experiment was subsequently repeated at the same CO conversion (11% − 136 °C). The same experimental protocol was carried out for the test in the presence of CO_2 by adding 0.2 vol% CO_2 in both gas feeds: $^{12}CO/{}^{12}CO_2/O_2/He \rightarrow {}^{13}CO/{}^{12}CO_2/O_2/ He/Kr/CH_4$. The gas flow composition from IR cell inlet/outlet was analyzed by micro-gas chromatography (Varian 490) and a quadrupole mass spectrometer (Pfeiffer QMS 200, 70 eV electronic impact) by recording He^+ (m/z = 4), $CH_4{}^+$ (m/z = 15), $^{12}CO^+$ (m/z = 28), $^{13}CO^+$ (m/z = 29), $^{12}CO_2{}^+$ (m/z = 44), $^{13}CO_2{}^+$ (m/z = 45) and Kr^+ (m/z = 84). The evolution of the adsorbed species on the catalytic material was analyzed by a Thermo Scientific Nicolet 6700 FTIR spectrometer (rapid-scan mode, 1 scan per spectra and resolution 2 cm^{-1}) equipped with a MCT detector. CO conversion (χ_{CO}) was calculated using the following Eq. (1):

$$\chi_{CO}(\%) = \frac{[CO_2]_t}{[CO]_0} \times 100 \quad (1)$$

The concentration of reversibly adsorbed CO (N_{CO}), active C-containing intermediates (N_C) leading to the formation of CO_2, and their respective surface coverage (θ) were calculated using the following Eqs. (2)−(4) based on material balances:

$$N_{CO}(\mu mol\ g_{cat}^{-1}) = \frac{F_T\ Y_{CO}^f\ (1-X_{CO})}{W} \int_0^{t_{s.s}} [Z_{CH_4}(t) - Z_{^{13}CO}(t)]\ dt \quad (2)$$

$$N_C(\mu mol\ g_{cat}^{-1}) = \frac{F_T\ Y_{^{13}CO_2}}{W} \int_0^{t_{s.s}} [Z_{^{13}CO}(t) - Z_{^{13}CO_2}(t)]\ dt \quad (3)$$

$$\theta_i = {N_i}/{N_{Pt,surf}} \quad (i = C, CO) \quad (4)$$

Where F_T is the total molar flow rate (μmols^{-1}) of the gas feed, Yf_{CO} is the mole fraction of CO in the feed, χ_{CO} is the CO conversion, W is the mass of catalyst (g), $Y_{^{13}CO_2}$ is the mole fraction of $^{13}CO_2$ at the outlet of the reactor in the new steady-state obtained, Z is the dimensionless concentration of a given gas-phase species, $t_{s.s}$ is the time at which the new steady-state is obtained under the ^{13}CO gas mixture,

and $N_{Pt,\,surf}$ is the molar amount of surface platinum per gram of catalyst (μmol Pt g_{cat}^{-1}) obtained based on the dispersion and loading values of Pt metal. The surface residence times (τ) of surface adsorbed species were calculated using Eqs. (5) and (6):

$$\tau_{CO}(s) = \int_0^{t_{s.s}} [Z_{CH_4}(t) - Z_{^{13}CO}(t)]\, dt \quad (5)$$

$$\tau_{C}(s) = \int_0^{t_{s.s}} [Z_{^{13}CO}(t) - Z_{^{13}CO_2}(t)]\, dt \quad (6)$$

The turnover frequencies, namely $TOF_{CO,\,ITK}$ and $TOF_{CO2,\,ITK}$ (s^{-1}), given by Eqs. (7) and (8) are based on the concentrations of active reaction intermediates found in the reaction path of CO_2 formation, N_{CO} and N_C, respectively.

$$TOF_{CO,ITK} = \frac{r_{CO}}{N_{CO}} \quad (7)$$

$$TOF_{CO_2,ITK} = \frac{r_{CO_2}}{N_C + N_{CO}} \quad (8)$$

where r_{CO} and r_{CO_2} are the steady-state rates of CO conversion and CO_2 formation in μmol g^{-1} s^{-1}, respectively.

3 Results and Discussions

3.1 Initial Catalyst Characterization

The catalyst exhibits a specific surface area of 232 m^2g^{-1} with a pore volume of 0.79 cm^3g^{-1} comparable to the area and pore volume obtained for the ɣ-Al_2O_3 support itself, 225 m^2g^{-1} and 0.76 cm^3g^{-1}, respectively. A loading of 0.82 wt% of Pt on alumina was determined using inductive coupled plasma optical emission spectroscopy (ICP-OES) analysis. Finally, H_2 chemisorption resulted in a dispersion of 68% corresponding to a mean Pt particle size of about 1.65 nm (Table S1 in supplementary material).

3.2 SSITKA-IR Studies for CO Oxidation

3.2.1 CO Oxidation Without CO_2 in the Reaction Mixture

Firstly, the oxidation of CO in an excess of O_2 has been conventionally carried out without the presence of CO_2 in the reaction feed. The normalized MS signals of ^{13}CO, $^{13}CO_2$ and CH_4 are presented in Fig. 1 as a function of time after applying a reactant isotopic switching from ^{12}CO to ^{13}CO at low conversion (χ_{CO} = 11% at 131 °C). It is worth noting that the ^{13}CO transient response curve lags behind that of the tracer (CH_4) due to the formation of reversibly adsorbed CO during oxidation reaction. The $^{13}CO_2$ transient response curve lags behind that of ^{13}CO indicating that, in theory, $^{13}CO_2$ passes through one or more adsorbed reaction intermediates after that of ^{13}CO before it forms $^{13}CO_2$. Based on the SSITKA theory (Eqs. 5 and 6), the integrations of observed delays between the response curves of CH_4 and ^{13}CO, then ^{13}CO and $^{13}CO_2$ provide the mean surface residence times τ of reversibly adsorbed CO (τ_{CO} = 5.0

s) and active intermediates (τ_C = 29.2 s), respectively. The latter values allow calculating the surface concentrations and coverages of each species using the Eq. 2 to 4. A concentration of 12.9 µmol of CO surface-adsorbed species (N_{CO}) per gram of catalyst is reached corresponding to a Pt surface coverage of about 45% (θ_{CO} = 0.45 in Table 1). In addition, a concentration of 9.6 µmolg^{-1} of C_x- adsorbed intermediate is determined corresponding to a surface coverage of 33% (θ_C = 0.33 in Table 1).

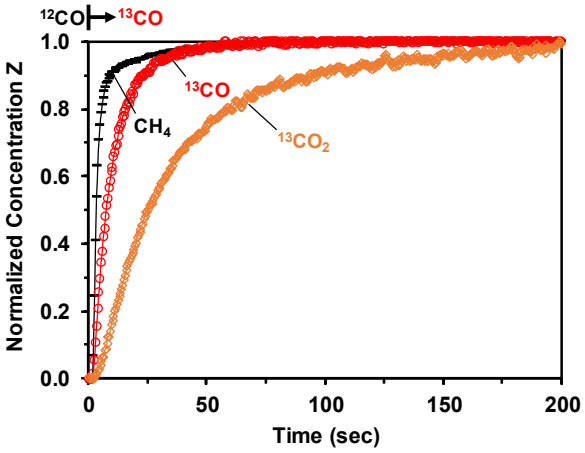

Fig. 1 − Normalized concentrations of CH_4, ^{13}CO and $^{13}CO_2$ obtained during the SSITKA transient ($^{12}CO/O_2/He \rightarrow {}^{13}CO/O_2/Kr/CH_4/He$) on Pt/Al_2O_3 at 131 °C (χ_{CO} = 11%)

The nature of the adsorbed species during the CO oxidation reactant isotopic transient on Pt/Al_2O_3 is followed by *operando* IR analysis. Two spectra are presented in Fig. 2 corresponding to the $^{12}CO+O_2$ and $^{13}CO+O_2$ flow stages at the steady state (1 min after isotopic reactant switching in case of ^{13}CO) and 131 °C.

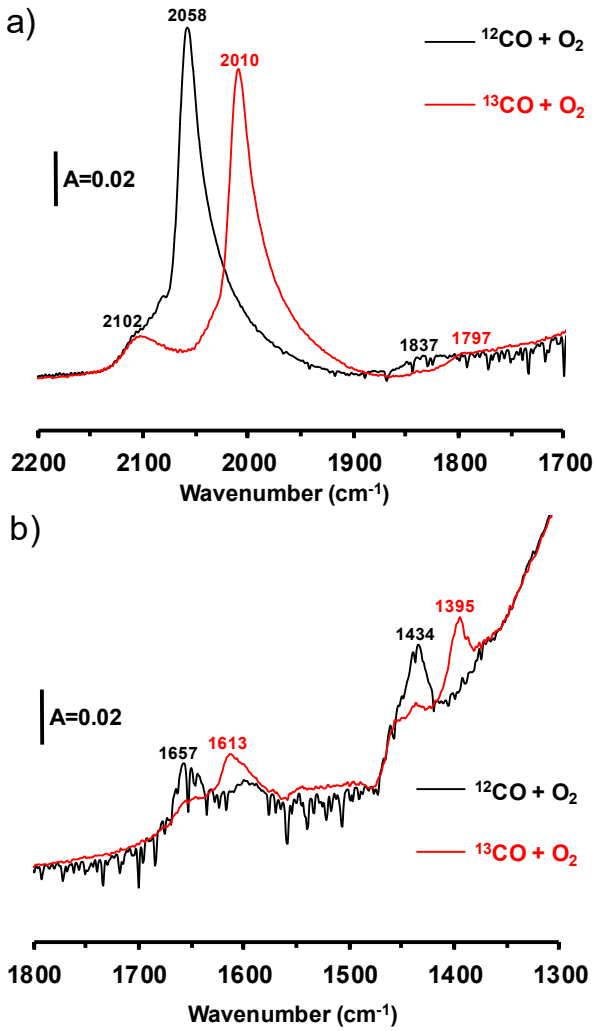

Fig. 2 − IR spectra recorded on Pt/Al_2O_3 during CO oxidation at 131 °C in the presence of $^{12}CO/O_2/He$ (black) and $^{13}CO/O_2/Kr/CH_4$ /He (red): (a) carbonyl region and (b) carbonate region

The black line in Fig. 2a, corresponding to the spectrum recorded in presence of ^{12}CO and O_2 in the carbonyl wavenumber region (2200 − 1700 cm^{-1}), shows a strong IR band at 2058 cm^{-1}. It corresponds to the stretching C ≡ O vibration of the ^{12}CO species linearly adsorbed on metallic Pt atom [16, 17]. A red shift of this band upon ^{13}CO exchange is observed, giving rise to a band at 2010 cm^{-1} corresponding to the ^{13}C-labelled linear carbonyls adsorbed on Pt^0. Carbonyls adsorbed on oxidized $Pt^{\delta+}$ are also observed on both spectra in Fig. 2a as a smaller IR bands around 2102 cm^{-1} [18]. No isotopic shift is shown in that case. The presence of bridged ^{12}CO carbonyl species adsorbed on two metallic platinum is also observed at 1837 cm^{-1} along with an isotopic ^{13}CO shift after the transient exchange at 1797 cm^{-1}. The carbonate region represented in Fig. 2b (1800 − 1300 cm^{-1}) can be decomposed with the bands at 1434 and 1657 cm^{-1} corresponding to the hydrogencarbonate species ν(OCO) asymmetric and ν(OCO) symmetric stretching vibrations, respectively [19]. A band near 1215 cm^{-1} corresponding to the bending δ(OH) vibrations as well as the stretching ν(OH) band at higher wavenumber would be expected for hydrogen-carbonates species. However, due to the low energy in these ranges, we were not

able to distinguish them. As for linear carbonyl species, a red isotopic shift is clearly spotted over the hydrogen-carbonates O = C = O bands. Upon exchange with ^{13}CO, the bands at 1434 and 1657 cm^{-1} shifts towards the bands at 1395 and 1613 cm^{-1}, respectively.

3.2.2 CO Oxidation in Presence of CO_2

The same experiment of CO oxidation with O_2 on Pt/Al_2O_3 catalyst has been repeated by adding, in that case, a significant amount of $^{12}CO_2$ in both SSITKA feeds ($^{12}CO/O_2/^{12}CO_2/He \rightarrow {}^{13}CO/O_2/^{12}CO_2/Kr/CH_4/He$). The normalized IR signals of ^{13}CO, $^{13}CO_2$ and CH_4 are represented as a function of time in Fig. 3 after applying the reactant isotopic switch at low conversion (χ_{CO} = 11% at 136 °C). In the presence of CO_2, the mean surface residence times of reversibly adsorbed CO (τ_{CO}) and active intermediates (τ_C) appear to be equal to 5.2 s and 3.6 s, respectively. While no significant effect of CO_2 is observed on τ_{CO}, the area between the ^{13}CO and $^{13}CO_2$ curves vanished quasi-completely leading to a drastic decrease of the τ_C value (Table 1). Consequently, new calculations of the surface concentration and coverage of CO on catalytic surface from MS signals appear to be quite similar to the value determined without the presence of CO_2, i.e. N_{CO} = 12.8 $\mu molg^{-1}$ and θ_{CO} = 0.45, unlike those obtained for C_x- adsorbed intermediate with N_C and θ_C dropping from 9.2 $\mu molg^{-1}$ and 0.33 to 1.4 $\mu molg^{-1}$ and 0.05 in presence of CO_2, respectively.

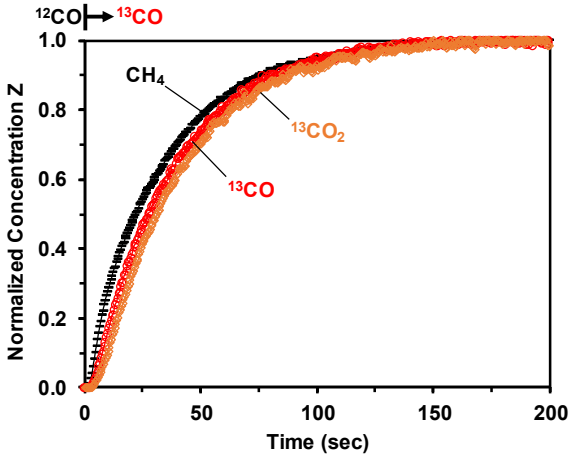

Fig. 3 − Normalized concentrations of CH_4, ^{13}CO and $^{13}CO_2$ obtained after the SSITKA transient in the presence of CO_2 in the feed ($^{12}CO/O_2/^{12}CO_2/He \rightarrow {}^{13}CO/O_2//^{12}CO_2/Kr/CH_4/He$) on Pt/Al_2O_3 at 136 °C (χ_{CO} = 11%)

The $TOF_{,ITK}$ were also calculated based on the concentration of reversibly adsorbed CO (N_{CO}) and the sum of the concentration N_{CO}+ N_C for TOF_{CO} and TOF_{CO2}, respectively (Eqs. 7 and 8, Table 1). It is worth noting that this calculation takes into account the active sites defined by SSITKA measurements (concentration of all the active species that truly participate in the formation of a given reaction product) and not the amount of Pt exposed surface sites determined by H_2- chemisorption as conventionally adopted for TOF determination [20]. As a direct result of the decrease of C_x- adsorbed intermediate

concentration (N_C), the $TOF_{CO2,\,ITK}$ increases by about 45% in the presence of CO_2 (from 0.015 s^{-1} to 0.027 s^{-1}) while the values of $TOF_{CO,\,ITK}$ remain similar in both cases.

Table 1 - Mean residence time τ, concentration N, surface coverage θ, and TOF of adsorbed CO reactant and active intermediates in CO_2 formation during SSITKA CO oxidation experiment with and without the presence of CO_2 in the feed on Pt/Al_2O_3

CO_{ads}	τ_{CO} (s)	N_{CO} (µmol/g)	θ_{CO}	$TOF_{CO,ITK}$ (s^{-1})
Without CO_2	5.0	12.9	0.45	0.20
With CO_2	5.2	12.8	0.45	0.19
C_x intermediates	τ_C (s)	N_C (µmol/g)	θ_C	$TOF_{CO2,ITK}$ (s^{-1})
Without CO_2	29.2	9.6	0.33	0.015
With CO_2	3.6	1.4	0.05	0.027

IR spectra analysis has also been performed to observe the evolution of adsorbed species on the catalytic surface after reactant exchange with ^{13}CO in the presence of CO_2. Figure 4 shows the IR spectra recorded during the $^{12}CO+O_2+^{12}CO_2$ and $^{13}CO+O_2+^{12}CO_2$ flow stages at the steady state (1 min after isotopic reactant switching in case of ^{13}CO) at 136 °C.

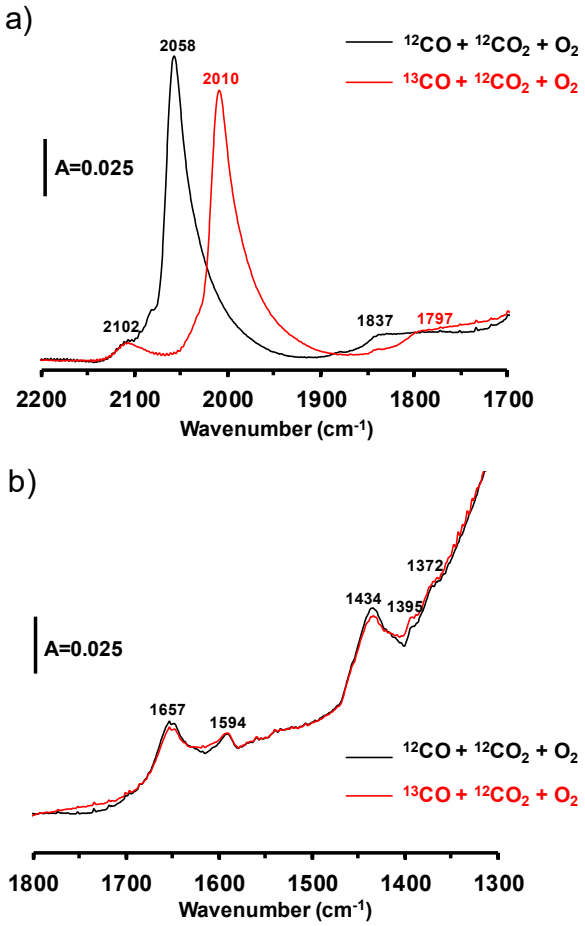

Fig. 4 − IR spectra recorded during CO oxidation at 136 °C in the presence of $^{12}CO/O_2/^{12}CO_2/He$ (black) and $^{13}CO/O_2/^{12}CO_2/Kr/CH_4/He$ (red): (a) carbonyl region and (b) carbonate region

The Fig. 4a shows the shift of the band at 2058 cm^{-1} in the carbonyl wavenumber region corresponding to ^{12}CO linear species adsorbed on metallic Pt towards the band of its labelled counterpart ^{13}CO adsorbed linear species at 2010 cm^{-1} as seen previously in Fig. 2. Once again, CO-$Pt^{\delta+}$ carbonyls are observed at 2102 cm^{-1} in both feeds without any isotopic shift effect while bridged carbonyls (Pt_2CO) are shifted from 1837 cm^{-1} to 1797 cm^{-1} regarding to $^{12}CO \rightarrow ^{13}CO$ reactant switch. Interestingly, in the presence of CO_2, the bands at 1434 cm^{-1} and 1657 cm^{-1} observed in the carbonate region (Fig. 4b) and attributed to O = C = O asymmetric and symmetric stretching vibrations of hydrogen-carbonate species are not shifted after reactant exchange to ^{13}CO. Other low-intensity non-shifted bands appear at 1594 cm^{-1}, 1395 cm^{-1} and 1372 cm^{-1} which can be assigned to OCO asymmetric stretching, C–H bending and OCO symmetric stretching vibrations of formate species formed on alumina surface, respectively [21, 22].

3.3 General Discussion

The interest for SSITKA-IR methodology is illustrated in this study for the discrimination of active and spectator species in a catalytic reaction. This combines both the observation of adsorbed species and the kinetic measurements during CO oxidation reaction at low conversion level (i.e. in chemical regime). The CO adsorption on Pt/Al_2O_3 mainly forms linear carbonyl type species adsorbed on metallic Pt^0 as observed at 2058 cm^{-1} (^{12}CO) and 2010 cm^{-1} (^{13}CO) with *operando* IR spectroscopy and in lower extent bridged carbonyl species on metallic Pt^0 (Fig. 2a). Moreover, after 1 min of the isotopic exchange, a complete vanish of the bands at 2058 cm^{-1} and 1837 cm^{-1} is observed which can be related to a high exchange rate and so high reactivity of CO adsorbed on Pt^0 during the experiment. This kinetic result is furthermore coherent with the gas phase evolution of ^{13}CO observed by mass spectrometry (Fig. 1) that reaches its maximum at around 60 s. In the meantime, no isotopic exchange during the $^{12}CO \rightarrow ^{13}CO$ SSITKA experiment is observed for carbonyls adsorbed on $Pt^{\delta+}$ suggesting a low reactivity and so their spectator nature in CO oxidation reaction at low temperature. An important lag was observed between the normalized ^{13}CO and $^{13}CO_2$ concentration curves indicating in theory the formation and participation of C-adsorbed reactive intermediates in the CO_2 production. According to the IR results (Fig. 2b) hydrogen-carbonate species seems to be the most serious contender to play the role of active intermediates in the CO oxidation reaction due to a high $^{12}C \rightarrow ^{13}C$ exchange rate at around 130 °C comparable to the rate of CO_2 product formation. The SSITKA-IR experiment in the presence of CO_2 in the feed gives additional information concerning the role of hydrogen-carbonate during CO oxidation. As a matter of fact, the simultaneous saturation of the catalyst surface with adsorbed CO_2 reduces by a factor of seven the amount of C-containing intermediate species (N_C) for the same CO conversion and reaction temperature when CO_2 is present in the reaction mixture. This result proves that the lag firstly

observed between ^{13}CO and $^{13}CO_2$ during the SSITKA experiment without CO_2 is due in reality to the re-adsorption of the CO_2, produced by the CO oxidation, on the surface of the catalyst rather than any intermediate formation or reactivity to form CO_2. IR spectra recorded in the presence of CO_2 also confirm this trend in which IR bands of hydrogen-carbonate species don't show any $^{12}C \rightarrow ^{13}C$ isotopic shift anymore. This observation clearly indicates that their formation is induced in that case by the adsorption of $^{12}CO_2$ already present in the gas feed rather than the conjugation of the reactants $^{13}CO+O_2$ with surface hydroxyls from alumina. The intermediate formation of hydrogen-carbonate during CO oxidation can therefore be definitely ruled out.

4 Conclusion

The formation of carbonyl and hydrogen-carbonate species was investigated on 0.82wt% Pt/Al_2O_3 during CO oxidation in lean conditions. The present work has provided fundamental insight into the role of hydrogen-carbonate species in CO oxidation reaction. SSITKA-IR technique has been applied for the first time to study this reaction. A fast shift of IR signals related to linear carbonyl and bridged carbonyl type species adsorbed on metallic Pt^0 was observed during the $^{12}CO+O_2$ and $^{13}CO+O_2$ transient exchange in absence and presence of CO_2 in the reaction mixture, confirming their high reactivity toward CO_2 formation contrary to carbonyls adsorbed on oxidized $Pt^{\delta+}$. The hydrogencarbonate species formed during CO oxidation reaction were finally proven to be inactive adsorbed species. The lag between the ^{13}CO and $^{13}CO_2$ observed on SSITKA normalized concentration curves was in fact explained by the readsorption of CO_2 product, formed from the CO oxidation, on the surface of the catalyst. This result was supported by the non-shifted IR bands of the hydrogen-carbonate species under $^{12}CO \rightarrow ^{13}CO$ transient exchange in presence of CO_2 in the gas feed.

Supplementary Information : https:// doi. org/ 10. 1007/ s11244- 022- 01722-2.

Acknowledgements The authors thank the Region "Hauts-de- France" (Grant STaRS 2019), Centrale Lille Institute, the Ministere de l'Enseignement Superieur et de la Recherche (CPER IRENE and CPER ECRIN) and the European Fund for Regional Economic Development for their financial support. ICP-OES analyses were performed in the « Spectrometrie par torche a plasma » platform of the Research Federation Michel-Eugene Chevreul hosted by the LASIRE laboratory.

Author Contributions All authors contributed to the study conception and design. Material preparation and data collection were performed by IH and NB. All authors participated to the methodology development and data analysis. The first draft of the manuscript was written by IH and all authors commented on previous versions of the manuscript. All authors read and approved the final manuscript. Data Availabilty The datasets generated during and/or analyzed during the current study are available from the corresponding author on reasonable request.

Declarations Conflict of interest The authors have no relevant financial or non-financial interests to disclose.

References

1. New WHO global air quality guidelines aim to save millions of lives from air pollution. https:// www. who. int/ news/ item/ 22- 09- 2021- new- who- global- air- quali ty- guide lines- aim- to- save- milli ons- of- lives- from- air- pollu tion. Accessed 8 Nov 2021

2. Casapu M, Fischer A, Ganzler AM et al (2017) Origin of the normal and inverse hysteresis behavior during CO oxidation over Pt/Al_2O_3. ACS Catal 7:343–355. https:// doi. org/ 10. 1021/ acsca tal. 6b027 09

3. Gao J, Tian G, Sorniotti A et al (2019) Review of thermal management of catalytic converters to decrease engine emissions during doi. org/ 10. 1016/j. applt herma leng. 2018. 10. 037

4. Carlsson P-A, Skoglundh M (2011) Low-temperature oxidation of carbon monoxide and methane over alumina and ceria supported platinum catalysts. Appl Catal B 101:669–67

5. https:// doi. org/ 10. 1016/j. apcatb. 2010. 11. 008 5. Heck RM, Farrauto RJ (2001) Automobile exhaust catalysts. Appl Catal A 221:443–457. https:// doi. org/ 10. 1016/ S0926- 860X(01) 00818-3

6. Shelef M, McCabe RW (2000) Twenty-five years after introduction of automotive catalysts: what next? Catal Today 62:35–50. https:// doi. org/ 10. 1016/ S0920- 5861(00) 00407-7

7. Al Soubaihi RM, Saoud KM, Dutta J (2018) Critical review of low-temperature CO oxidation and hysteresis phenomenon on heterogeneous catalysts. Catalysts 8:660. https:// doi. org/ 10. 3390/ catal 81206 60

8. Salomons S, Hayes RE, Votsmeier M et al (2007) On the use of mechanistic CO oxidation models with a platinum monolith catalyst. Appl Catal B 70:305–313. https:// doi. org/ 10. 1016/j. apcatb. 2006. 01. 022

9. Salomons S, Votsmeier M, Hayes RE et al (2006) CO and H_2 oxidation on a platinum monolith diesel oxidation catalyst. Catal Today 117:491–497. https:// doi. org/ 10. 1016/j. cattod. 2006. 06. 001

10. Carlsson P-A, Osterlund L, Thormahlen P et al (2004) A transient in situ FTIR and XANES study of CO oxidation over Pt/Al_2O_3 catalysts. J Catal 226:422–434. https:// doi. org/ 10. 1016/j. jcat. 2004. 06. 009

11. Newton MA, Ferri D, Smolentsev G et al (2015) Room-temperature carbon monoxide oxidation by oxygen over Pt/Al_2O_3 mediated by reactive platinum carbonates. Nat Commun 6:8675. https:// doi. org/ 10. 1038/ ncomm s9675

12. Newton MA (2017) Time resolved operando X-ray techniques in catalysis, a case study: CO oxidation by O_2 over Pt surfaces and alumina supported Pt catalysts. Catalysts 7:58. https://d oi.o rg/1 0. 3390/ catal 70200 58

13. Newton MA, Ferri D, Smolentsev G et al (2016) Kinetic studies of the Pt carbonate-mediated, room-temperature oxidation of carbon monoxide by oxygen over Pt/Al_2O_3 using combined, timeresolved XAFS, DRIFTS, and mass spectrometry. J Am Chem Soc 138:13930–13940. https:// doi. org/ 10. 1021/ jacs. 6b068 19

14. Burch R, Shestov AA, Sullivan JA (1999) A steady-state isotopic transient kinetic analysis of the NO/O_2/H_2 reaction over Pt/SiO_2 catalysts. J Catal 188:69–82. https:// doi. org/ 10. 1006/ jcat. 1999. 2653

15. Ledesma C, Yang J, Chen D, Holmen A (2014) Recent approaches in mechanistic and kinetic studies of catalytic reactions using SSITKA Technique. ACS Catal 4:4527–4547. https:// doi. org/ 10. 1021/ cs501 264f

16. Bourane A, Dulaurent O, Chandes K, Bianchi D (2001) Heats of adsorption of the linear CO species on a Pt/Al_2O_3 catalyst using FTIR spectroscopy: comparison between TPD and adsorption equilibrium procedures. Appl Catal A 214:193–202. https:// doi. org/ 10. 1016/ S0926- 860X(01) 00483-5

17. Bourane A, Bianchi D (2003) Oxidation of CO on a Pt/Al_2O_3 catalyst: from the surface elementary steps to light-off tests: IV. Kinetic study of the reduction by CO of strongly adsorbed oxygen species. J Catal 220:3–12. https:// doi. org/ 10. 1016/ S0021- 9517(03) 00267-7

18. Bourane A, Derrouiche S, Bianchi D (2004) Impact of Pt dispersion on the elementary steps of CO oxidation by O_2 over Pt/ Al_2O_3 catalysts. J Catal 228:288–297. https:// doi. org/ 10. 1016/j. jcat. 2004. 08. 020

19. Ojala S, Bion N, Rijo Gomes S et al (2010) Isotopic oxygen exchange over Pd/Al_2O_3 catalyst: study on $C^{18}O_2$ and $^{18}O_2$ exchange. Chem- CatChem 2:527–533. https:// doi. org/ 10. 1002/ cctc. 20100 0033

20. Vasiliades MA, Kalamaras CM, Govender NS et al (2019) The effect of preparation route of commercial Co/γ-Al_2O_3 catalyst on important Fischer-Tropsch kinetic parameters studied by SSITKA and CO-DRIFTS transient hydrogenation techniques. J Catal 379:60–77. https:// doi. org/ 10. 1016/j. jcat. 2019. 09. 008

21. Lorito D, Paredes-Nunez A, Mirodatos C et al (2016) Determination of formate decomposition rates and relation to product formation during CO hydrogenation over supported cobalt. Catal Today 259:192–196. https:// doi. org/ 10. 1016/j. cattod. 2015. 06. 027

22. McInroy AR, Lundie DT, Winfield JM et al (2005) The application of diffuse reflectance infrared spectroscopy and temperatureprogrammed desorption to investigate the interaction of methanol on η-Alumina. Langmuir 21:11092–11098. https:// doi. org/ 10. 1021/ la051 429c